
Contents

1	Introduction	1
2	A dark sector with $U(1)_{B-L}$	2
3	Parametrization of the physical states	5
3.1	Neutrino masses	6
4	Phenomenology	7
4.1	Constraints from Higgs decays	8
4.2	Direct detection	10
4.3	Dark Matter relic abundance	11
4.4	Constraints from indirect searches and CMB	14
4.5	Self-interacting Dark Matter	17
5	Results	19
6	Conclusions and outlook	21

1 Introduction

The study of the dark Universe is one of the best handles to understand what lies beyond the Standard Model (SM), particularly possible connections between Dark Matter and other sectors. The SM neutrino sector is especially interesting, as the observation of neutrino masses already points to new physics beyond the SM, possibly in the form of massive right-handed neutrinos. This raises the question whether these two new forms of massive particles, Dark Matter and right-handed neutrinos, are somewhat linked.

A very minimal possibility would be that of right-handed neutrinos constituting the Dark Matter of the Universe [1]. Yet, this option is tightly constrained in a region of small mixing with active neutrinos and mass around the keV, which will be explored in upcoming experiments and potentially excluded, see [2] for a recent review on the subject.

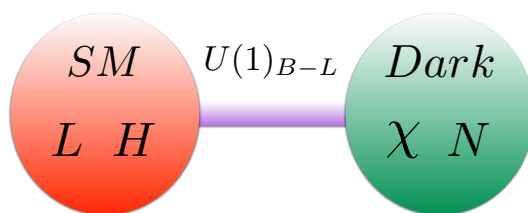
In this paper we propose a different scenario, where sterile neutrinos and a fermionic Dark Matter particle would have a common origin within a dark sector. These dark fermions would exhibit couplings to a dark scalar, which would bring a source of Majorana masses. The right-handed neutrinos would mix with active neutrinos, providing a link to the SM, which Dark Matter would inherit via exchanges of the dark scalar. Additionally, the dark scalar could couple to the SM via a Higgs portal, providing Dark Matter yet another mechanism to communicate with the SM. In this paper we choose the rather natural option of charging the dark sector under $U(1)_{B-L}$, but another minimal choice would be to assume an exact symmetry of the dark sector which stabilizes the lightest dark

particle and allows to communicate with the SM via the right-handed neutrinos, singlets under both the SM and the dark group, see [3, 4] and [5].

The paper is organized as follows. After presenting the set-up of our model in section 2, and the consequences of the breaking of $U(1)_{B-L}$ in the scalar sector in section 3, we move onto the phenomenology of the model in section 4. The study of Higgs decays and direct detection in sections 4.1 and 4.2, does lead to strong constraints on the mixing between the dark scalar and the Higgs. How Dark Matter can satisfy the observed relic abundance is explored in section 4.3, and the correlation with indirect detection in section 4.4. We discuss the implications of a strongly self-interacting Dark Matter in this model in section 4.5, just before moving onto summarizing our findings in section 5. We conclude in section 6 by providing a summary of the results and outlook of possible new directions of investigation.

2 A dark sector with $U(1)_{B-L}$

We consider the following set-up: we extend the SM with a complex scalar field, ϕ and n chiral (RH) fermion fields, Ψ_R . All these new fields are SM singlets, and charged under a global $U(1)$ symmetry which can be identified with $U(1)_{B-L}$, so that $L_\phi = 2$ and $L_{\Psi_R} = 1$.¹



Moreover, we assume that (for the reasons explained below) some of the dark fermions have vanishing or suppressed coupling to the SM singlet operator $\bar{L}_L H$, so they could be stable (or cosmologically stable); we will denote such stable fermion(s) by χ_R , as opposed to the rest of the dark fermions, which we will call N_R .

Communication between the Standard Model fields and the new singlet sector (ϕ, Ψ_R) is determined by the $U(1)_{B-L}$ charges and the requirement of renormalizability of the interactions. The relevant part of the Lagrangian reads:

$$\begin{aligned} \mathcal{L} \supset & \mu_H^2 H^\dagger H - \lambda_H (H^\dagger H)^2 + \mu_\phi^2 \phi^\dagger \phi - \lambda_\phi (\phi^\dagger \phi)^2 - \lambda_{H\phi} (H^\dagger H) (\phi^\dagger \phi) \\ & - \left(\frac{\lambda_{\chi ab}}{\sqrt{2}} \phi \bar{\chi}_{Ra} \chi_{Rb}^c + h.c. \right) - \left(\frac{\lambda_{N ab}}{\sqrt{2}} \phi \bar{N}_{Ra} N_{Rb}^c + h.c. \right) - (Y_{\alpha a} \bar{L}_L^\alpha H N_{Ra} + h.c.) \end{aligned} \quad (2.1)$$

¹Note that $U(1)_{B-L}$ is the only anomaly-free global symmetry in the SM. Therefore, extensions of the SM including a *gauged* $U(1)_{B-L}$ have been considered in various contexts, and in particular in scenarios where the breaking appears at low-scale (e.g. [6–9]).

where $\alpha = e, \mu, \tau$ denotes lepton flavour, a, b refers to the different dark fermion species and the Yukawa coupling matrices λ_χ, λ_N are symmetric.

The coupling between the Higgs and the complex scalar ϕ , $\lambda_{H\phi}$, is a generalized *Higgs portal* coupling, whereas the direct coupling between the right-handed fermions N_R and the SM via the mixing term $Y_{\alpha a}$ leads to masses for the active neutrinos. The Yukawa coupling between the dark scalar and dark fermions λ_χ, λ_N generates a Majorana mass for the χ fields and sterile neutrinos provided ϕ develops a vev. Details on neutrino mass generation in this set-up can be found in section 3.1.

So far, we have described a new sector linked to the origin of neutrino masses. We now consider whether this sector could also describe Dark Matter. In our set-up there are two possible candidates 1.) the right-handed fermions χ_{Ra} , and/or 2.) a component of the complex scalar field ϕ . We discuss in turn each possibility.

Fermionic Dark Matter: possible mechanisms to ensure stability of the dark fermions χ_R could be:

1. *Z₂ symmetry:* the simplest possibility is that the fermions χ_R are odd under an exact Z_2 symmetry, while all the SM particles, the singlet scalar ϕ and the remaining fermions N_R are even. Then, the Yukawa coupling of χ_R to SM leptons will be forbidden, resulting on a stable sterile neutrino Dark Matter.
2. *Compositeness:* the dark sector is a low-energy description of a new strongly coupled sector (charged under the global $U(1)_{B-L}$), with the dark particles bound states of the strong dynamics. Mixing between the SM operator $\bar{L}_L^\alpha H$ and fermionic bound states \mathcal{O}^a with lepton number are allowed, but the strength of this mixing is determined by the anomalous dimension of \mathcal{O}^a . One could also describe this set-up in terms of a holographic dual, where operators from a strongly coupled sector like \mathcal{O}^a are represented by states living in more than 4D, $\mathcal{O}^a(x) \rightarrow \chi_R(x, z)$, with z is the extra dimensional coordinate. In this holographic picture, the SM particles (lepton doublets, Higgs) are localized at some distance from where the fields χ_R have their main support. The values of $Y_{\chi\alpha a}$ are obtained via dimensional reduction from 5D to 4D, namely computing overlaps of the wavefunctions of the Higgs, lepton doublets and dark fermions [10, 11]

$$Y_{\chi\alpha a} \propto \int dz f_H(z) f_{L^\alpha}(z) f_{\chi_{Ra}}(z). \tag{2.2}$$

In warped geometries, $\mathcal{O}(1)$ differences in localization parameters can lead to exponential hierarchies among the different entries in $Y_{\chi\alpha a}$ [12] and hence (meta)stability of some dark fermions.

3. *Exotic lepton number:* if there are at least two Weyl fermions in the dark sector, they could have lepton number different from ± 1 , so that the Yukawa interaction $\bar{L}_L^\alpha H \chi_{Ra,b}$ is forbidden but the coupling $\phi \bar{\chi}_{Ra} \chi_{Rb}^c$ is allowed provided $L_a + L_b = -2$. This scenario leads to Dirac Dark Matter particle, and has been explored in [13] in the context of the Zee-Babu model for neutrino masses.

4. *Different dark sector representations:* the dark sector could have further symmetry structure (more complex than the simple Z_2 symmetry described above), so that some of the chiral fermions are singlets under the dark symmetry group and thus can couple to $\bar{L}_L^\alpha H$, while χ_{Ra} may transform non trivially under the dark group. Then, $\phi \bar{\chi}_{Ra} \chi_{Ra}^c$ is invariant and thus allowed, but the Yukawa coupling with the SM fermions is forbidden by the dark symmetry.

In this paper we assume that either mechanism 1 or 3 are at work, and we discuss the phenomenology of these two minimal realizations. In the case of an additional dark sector symmetry, if it is global the only difference will be an extra factor in the annihilation cross sections of section 4.3, related to the dimension of the representation to which χ_R belongs, so our results can be easily re-scaled; however, if the dark symmetry is gauged, Dark Matter self-interactions could modify some of our findings.

Scalar Dark Matter: the imaginary part of the complex field (the so-called Majoron, η) could be a Dark Matter candidate [6, 14] provided it acquires a mass, e.g. via non-perturbative gravitational effects which break the global symmetry [15, 16]. For a recent review on the subject see [17].

A massive Majoron decays at tree level to a pair of light neutrinos with a rate that scales as [16]:

$$\Gamma(\eta \rightarrow \nu\nu) = \frac{m_\eta}{8\pi} \left(\frac{m_\nu}{v_\phi} \right)^2, \tag{2.3}$$

where m_ν is the mass scale of ordinary neutrinos and v_ϕ the scale of $U(1)_{B-L}$ spontaneous breaking. Therefore, for instance if $m_\eta \lesssim 10$ keV and $v_\phi \gtrsim 10^8$ GeV, the lifetime of the Majoron can be large enough for it to be stable on cosmological scales, while for v_ϕ in the TeV range the Majoron decays very fast.

Moreover, the massive Majoron might also decay into two photons at the loop level, although this mode is model-dependent. While it does not occur in the minimal singlet Majoron scenario that we are considering, it is induced at one loop in the more general see-saw model which includes also a triplet scalar field coupled to the SM lepton doublets [18], and it could also be present if the dark sector contains other chiral fermion representations charged under the SM gauge group with masses of order $\Lambda \gg v_\phi$, which would make the global symmetry $U(1)_{B-L}$ anomalous. Current experimental bounds on pseudo-Goldstone bosons with $\text{BR}(\eta \rightarrow \gamma\gamma) \sim 1$ imply that it can have a lifetime longer than $\sim 10^{20}$ years if its mass is $m_\eta \lesssim 100$ keV, while for heavier masses, $m_\eta \gtrsim 10$ MeV, the lifetime has to be shorter than one minute [19].

Both Dark Matter candidates, a keV scale sterile neutrino and a massive Majoron have received much attention in the literature, so we do not explore such possibilities any further in this paper. Instead, we focus on the fermionic Dark Matter scenario extending the study to larger masses, in the typical WIMP range, which to our knowledge has not been considered up to now. It has been studied in the framework of gauged $U(1)_{B-L}$, however then there is also a new Z' gauge boson and constraints from direct searches set a lower bound on the scale of $U(1)_{B-L}$ symmetry breaking of order few TeV [20]. As



Figure 1. (Left) Decay of the Higgs to two Majorons η via the mixing of the Higgs with ρ . (Right) Exotic decay of the Higgs into a light neutrino and a dark fermion via their mixing.

The mixing of the two scalars, the Higgs h and ρ , is tightly constrained by 1.) limits on the Higgs invisible width BR_{inv} and global fits on Higgs properties as discussed on section 4.1 and 2.) limits on direct detection (DD) from LUX [25, 26], and XENON1T [27] in the near future, see section 4.2.

The mixing of the dark fermions N and the left-handed SM neutrinos via their coupling to the Higgs produces a spectrum of massive neutrinos (see section 3.1), but also leads to exotic decays of the Higgs to a dark fermion and a light neutrino. These are discussed in section 4.1.

The interactions and masses of the dark fermions, Dark Matter χ and heavy neutrinos N , and the dark scalar ρ can be probed in several ways. In section 4.3 we explain constraints from relic abundance $\Omega_{\text{DM}}h^2$ from Planck [28, 29], which provide information on the interplay among the competing annihilation processes, mainly the balance between the right-handed neutrino channel $\chi\chi \rightarrow NN$ and the annihilation to dark scalars, $\chi\chi \rightarrow \eta\rho$ and $\rightarrow \eta\eta$. Direct detection (DD) would provide complementary information, but it relies on the mixing of the dark scalar to the Higgs as mentioned above. Finally, annihilation of Dark Matter today could lead indirect detection (ID) signatures, namely features in the gamma-ray spectrum and signals in neutrino telescopes. These are discussed in section 4.4.

Finally, properties of the Majoron dark scalar η can be probed by imprints in the CMB, such as N_{eff} (see section 4.4) as well as by constraints on self-interacting Dark Matter (SIDM) which come from lensing and numerical simulations.

To deduce the constraints, we perform a simple Monte Carlo scan over the parameters in logarithmic scale, restricting the values of the couplings to the perturbative range, $\lambda_{\chi, N, \phi} \lesssim \mathcal{O}(1)$ and the masses in the region of interest, m_χ & m_N from 1 GeV to 2 TeV, m_ρ from 0.1 GeV to 10 TeV and $|\theta|$ from 10^{-4} to π . For the numerical implementation we made use of LanHep [30] and micrOMEGAs [31] in order to obtain the correct relic abundance, Higgs decays and today's annihilation cross section. We calculate 10^6 points that match the *Planck* constraint on the Dark Matter abundance at 3σ [29], namely $\Omega h^2 = 0.1198 \pm 0.0045$.

4.1 Constraints from Higgs decays

In the two scenarios that we consider, the enlarged fermion and scalar sectors lead to new decays of the Higgs boson, h as shown in figure 1. ATLAS and CMS constrain the invisible

Higgs decay branching fraction as [32, 33]

$$\text{BR}_{\text{inv}} = \frac{\Gamma_{\text{inv}}}{\Gamma_{\text{inv}} + \Gamma_{\text{SM}}} < 0.23 \quad (95\% \text{CL}), \quad (4.1)$$

where the SM Higgs width is $\Gamma_{\text{SM}} \approx 4 \text{ MeV}$.

The mixing of the two CP-even real scalars induce the following decay channels:

$$\Gamma(h \rightarrow \eta\eta) = \frac{m_h^3}{32\pi v_\phi^2} \sin^2 \theta \quad (4.2)$$

$$\Gamma(h \rightarrow \rho\rho) = \frac{(m_h^2 + 2m_\rho^2)^2}{128\pi m_h^2 v_H^2 v_\phi^2} \sqrt{m_h^2 - 4m_\rho^2} (v_H \cos \theta - v_\phi \sin \theta)^2 \sin^2 2\theta \quad (4.3)$$

$$\Gamma(h \rightarrow \chi\chi) = \frac{\lambda_\chi^2}{16\pi} \left(1 - \frac{4m_\chi^2}{m_h^2}\right)^{3/2} m_h \sin^2 \theta \quad (4.4)$$

$$\Gamma(h \rightarrow NN) = \frac{\lambda_N^2}{16\pi} \left(1 - \frac{4m_N^2}{m_h^2}\right)^{3/2} m_h \sin^2 \theta, \quad (4.5)$$

where we have neglected contributions to $h \rightarrow NN$ from the mixing among sterile and active neutrinos. This is justified by the smallness of the mixing, $\mathcal{O}(\sqrt{m_\nu/m_N})$. The decay to SM particles is modified as

$$\Gamma(h \rightarrow \text{SM particles}) = \cos^2 \theta \Gamma_{\text{SM}}. \quad (4.6)$$

These global modifications of the Higgs couplings are equivalent to the well-studied case of mixing of the Higgs with a singlet and are well constrained [32, 33]. In the low m_ρ region, the constraints one obtains from the invisible width is of the same order as this overall shift, hence below we use BR_{inv} as experimental input. Note that the corresponding expressions for ρ decays widths are obtained by exchanging $\sin \theta \rightarrow \cos \theta$ and $m_h \rightarrow m_\rho$.

From the equation of the h decay rate into two Majorons, $\Gamma(h \rightarrow \eta\eta)$, the experimental upper limit on the invisible decay width of the Higgs boson leads to the following upper bound on the mixing angle θ [34]:

$$|\tan \theta| \lesssim \sqrt{\frac{32\pi v_\phi^2 \Gamma_{\text{Higgs}}^{\text{SM}} \text{BR}_{\text{inv}}}{m_h^3 (1 - \text{BR}_{\text{inv}})}} \sim 2.2 \times 10^{-3} \left(\frac{v_\phi}{10 \text{ GeV}}\right) \quad (4.7)$$

Including the other decay processes, when kinematically allowed, would reduce further the upper limit.

The Yukawa interaction term $Y\bar{L}HP_R N$ also leads to novel Higgs decay channels into neutrinos, even in the absence of mixing between the CP-even scalars. The corresponding decay width reads (for $\theta = 0$):

$$\Gamma(h \rightarrow \nu_i \nu_j) = \frac{\omega}{8\pi m_h} \lambda^{1/2}(m_h^2, m_i^2, m_j^2) \left[S \left(1 - \frac{(m_i + m_j)^2}{m_h^2}\right) + P \left(1 - \frac{(m_i - m_j)^2}{m_h^2}\right) \right], \quad (4.8)$$

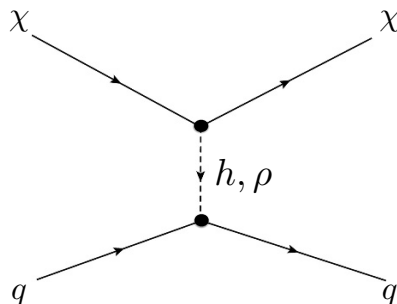


Figure 2. Dark matter interaction relevant to direct detection constraints.

where $\lambda(a, b, c)$ is the standard kinematic function, $w = 1/n!$ for n identical final particles and the scalar and pseudoscalar couplings are:

$$S = \frac{1}{v_H^2} [(m_i + m_j) \text{Re}(C_{ij})]^2, \quad P = \frac{1}{v_H^2} [(m_j - m_i) \text{Im}(C_{ij})]^2, \quad (4.9)$$

with C_{ij} defined in eq. (3.16). The largest branching ratio is for the decay into one light and one heavy neutrino [35]:

$$\Gamma(h \rightarrow \nu N) = \frac{m_N^2}{8\pi v_H^2} \left(1 - \frac{m_N^2}{m_h^2}\right)^2 m_h |C_{\nu N}|^2. \quad (4.10)$$

The attainable values for the above branching fractions have been analyzed in [35], for the case of two heavy neutrinos, parameterizing the Yukawa couplings in terms of the observed light neutrino masses and mixing angles, and a complex orthogonal matrix. After imposing the relevant constraints from neutrinoless double beta decay, lepton flavour violating processes and direct searches of heavy neutrinos, they find that branching ratios of $h \rightarrow \nu N$ larger than 10^{-2} are generally ruled out for heavy neutrino masses $m_N \leq 100$ GeV, and typically they are much smaller, due to the tiny Yukawa couplings required to fit light neutrino masses with sterile neutrinos at the electroweak scale. Therefore, the contribution of such decay modes to the Higgs decay width is negligible, and they do not alter the bounds discussed above.

4.2 Direct detection

In this scenario, Dark Matter scattering on nuclei relevant for direct Dark Matter detection is mediated via t -channel exchange by the CP even mass eigenstates, h, ρ and it is spin-independent, see figure 2.

The elastic scattering cross section of χ off a proton is given by [19]:

$$\sigma_{\chi p} = C^2 \frac{(\lambda_\chi \sin 2\theta)^2}{4\pi v_H^2} \frac{m_p^4 m_\chi^2}{(m_p + m_\chi)^2} \left(\frac{1}{m_h^2} - \frac{1}{m_\rho^2}\right)^2, \quad (4.11)$$

where m_p stands for the proton mass and $C \simeq 0.27$ is a constant that depends on the nuclear matrix element [31].

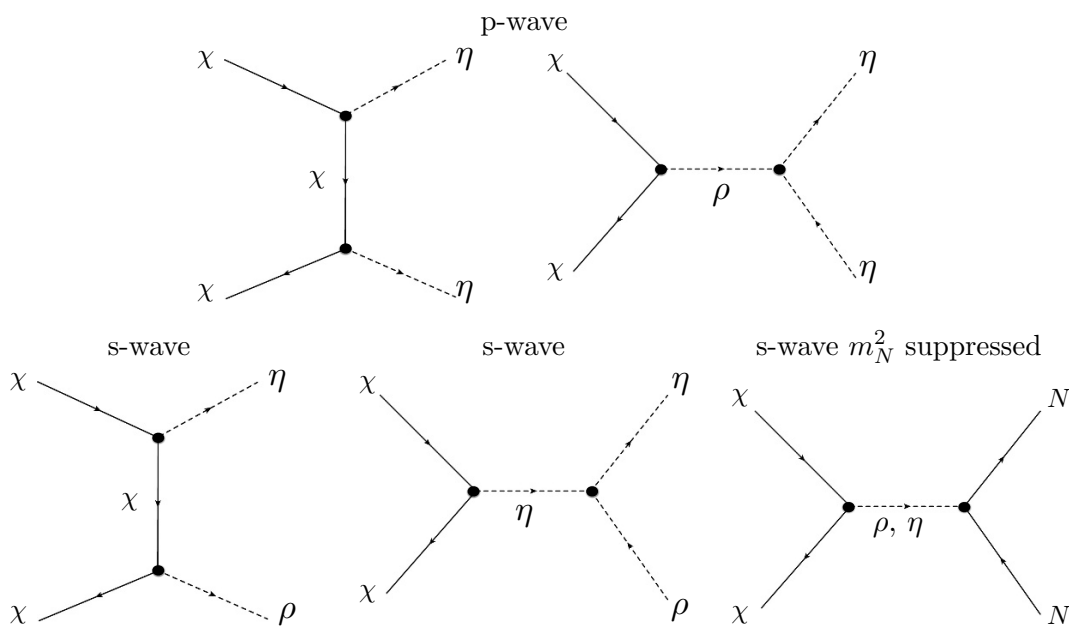


Figure 4. Diagrams relevant to the relic abundance computation.

the dominant annihilation channels, involving the new scalars ρ, η as well as the sterile neutrinos N , see figure 4. For simplicity, in the following we will only consider one generation of right-handed neutrinos, but extending the discussion to more generations will be straightforward. Therefore, in order to reduce the large number of free parameters in this analysis we set the mixing angle $\theta = 0$, and we scan over the remaining independent variables, chosen to be m_χ, m_N, m_ρ and λ_χ .

There are two channels with s-wave annihilation cross-section, the production of two right-handed neutrinos and the final state $\eta\rho$,

$$\begin{aligned} \sigma_{\chi\chi \rightarrow \rho\eta} v_{\text{rel}} &= \frac{m_\chi^2}{1024\pi v_\phi^4} (4 - r_\rho^2)^3 + \mathcal{O}(v_{\text{rel}}^2), \\ \sigma_{\chi\chi \rightarrow NN} v_{\text{rel}} &= \frac{m_N^2}{64\pi v_\phi^4} \sqrt{1 - r_N^2} + \mathcal{O}(v_{\text{rel}}^2). \end{aligned} \tag{4.12}$$

Other possible channels are p-wave suppressed,

$$\begin{aligned} \sigma_{\chi\chi \rightarrow \eta\eta} v_{\text{rel}} &= \frac{m_\chi^2}{192\pi v_\phi^4} \frac{8 + r_\rho^4}{(r_\rho^2 - 4)^2} v_{\text{rel}}^2, \\ \sigma_{\chi\chi \rightarrow \rho\rho} v_{\text{rel}} &= \frac{m_\chi^2}{384\pi v_\phi^4} \frac{\sqrt{1 - r_\rho^2}}{(r_\rho^2 - 4)^2} (144 - 32r_\rho^2) v_{\text{rel}}^2 + \mathcal{O}(r_\rho^4). \end{aligned} \tag{4.13}$$

Here $v_{\text{rel}} = 2\sqrt{1 - 4m_\chi^2/s}$ is the relative velocity of the Dark Matter in the center of mass frame and the ratios are given by $r_\rho = m_\rho/m_\chi$ and $r_N = m_N/m_\chi$.

As the annihilation channel into sterile neutrinos is not velocity suppressed, it can be comparable to the scalar channels, $\chi\chi \rightarrow \eta\eta, \rho\rho, \eta\rho$, which alike the NN channel, are not

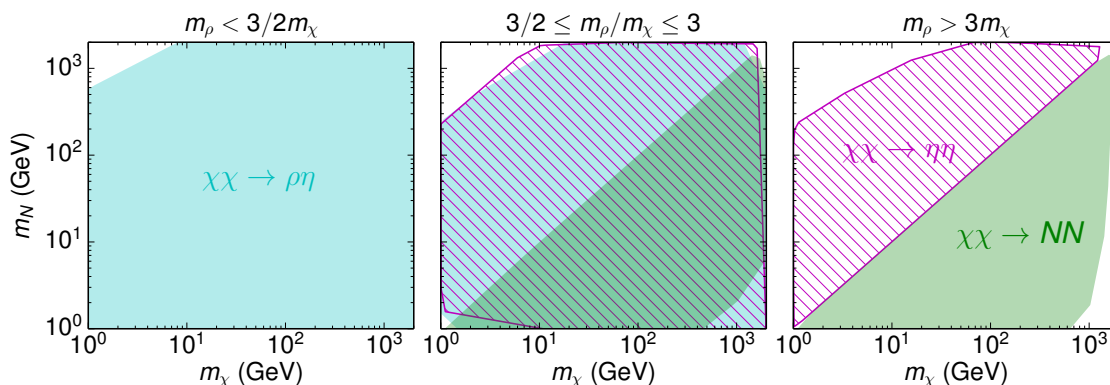


Figure 5. Allowed values of dark fermion masses, m_χ and m_N . The different colours correspond to regions in parameter space in which the annihilation channel constitutes more than 60% of the total cross section for $v = 10^{-3}c$, as relevant for indirect detection.

vanishing even in the case of zero $h - \rho$ mixing. We find that there is a significant fraction of the parameter space of the model in which the annihilation channel into NN is relevant, and even dominant. This is shown in figure 5, where allowed values of dark fermion masses, m_χ and m_N are depicted, with different colours corresponding to regions with dominance of one channel in the annihilation cross section for $v = 10^{-3}c$, as relevant for the calculation of direct detection constraints. The three panels of figure 5 correspond to different ranges of the dark scalar mass, m_ρ . In particular, in the middle panel we have singled out the region $3/2 \leq m_\rho/m_\chi \leq 3$, where the annihilation into $\eta\eta$ is resonantly enhanced.

On the other hand, the annihilation channel $\eta\rho$ tends to dominate when kinematically accessible (i.e., in the region $m_\rho < 2m_\chi$, since we are neglecting the mass of the Majoron, m_η), as it is parametrically enhanced respect to the other s-wave channel into right-handed neutrinos by $(m_\chi/m_N)^2$. Finally, in the range $m_\rho > 2m_\chi$, the two channels NN and $\eta\eta$ compete: the former dominates when $m_N \lesssim m_\chi$ and $m_\rho > 3m_\chi$, while in the resonance region $3/2 \leq m_\rho/m_\chi \leq 3$ we find that any of the two annihilation channels may dominate, as well as the $\eta\rho$ if open (central panel).

Interestingly, the $\eta\eta$ channel could have dominated the dynamics at freeze out, with the NN channel playing an spectator role, but for the usual velocities that the Dark Matter particles have in the galactic halo $v \simeq 10^{-3}c$, the NN channel could dominate the Dark Matter annihilation at later times. However, even if dominant, the cross section may be too small to lead to any indirect detection signature (see figure 8).

Notice that due to the $U(1)_{B-L}$ symmetry, there is a non trivial relation between the mass of the sterile neutrinos and the Dark Matter annihilation cross section into them, since both are proportional to the coupling λ_N . As a consequence, when the sterile neutrinos are very light, and the phase space is more favourable, the coupling is too small and the annihilation into sterile neutrinos is suppressed. On the other hand, if the coupling λ_N is large, the sterile neutrinos are too heavy, and this annihilation channel is phase space suppressed or even forbidden. Due to this relation between sterile neutrino masses and coupling to the scalar ϕ , the Dark Matter annihilation cross section into NN , although

W, Z , whose partial widths read [37]:

$$\Gamma(N \rightarrow \nu q \bar{q}) = 3 AC_{NN} [2(a_u^2 + b_u^2) + 3(a_d^2 + b_d^2)] f(z) \quad (4.16)$$

$$\Gamma(N \rightarrow 3\nu) = AC_{NN} \left[\frac{3}{4} f(z) + \frac{1}{4} g(z, z) \right] \quad (4.17)$$

$$\Gamma(N \rightarrow \ell q \bar{q}) = 6 AC_{NN} f(w, 0) \quad (4.18)$$

$$\Gamma(N \rightarrow \nu \ell \bar{\ell}) = AC_{NN} [3(a_e^2 + b_e^2) f(z) + 3f(w) - 2a_e g(z, w)] \quad (4.19)$$

where C_{NN} is defined in eq. (3.16),

$$A \equiv \frac{G_F^2 m_N^5}{192 \pi^3}, \quad (4.20)$$

a_f, b_f are the left and right neutral current couplings of the fermions ($f = q, \ell$), the variables z, w are given by

$$z = (m_N/m_Z)^2, \quad w = (m_N/m_W)^2, \quad (4.21)$$

and the functions $f(z), f(w, 0)$ and $g(z, w)$ can be found in [38].

Assuming no strong cancellations in the mixing matrix U , we expect $C_{NN} \sim m_\nu/m_N$, so from the equations above we can estimate the ratio between the total decay width to three SM particles and the invisible decay width to $\nu\eta$, given by eqs. (4.14):

$$\frac{\Gamma(N \rightarrow 3 \text{ SM})}{\Gamma(N \rightarrow \nu\eta)} \sim \frac{1}{\pi^2} \left(\frac{m_N}{v_H} \right)^2 \left(\frac{v_\phi}{v_H} \right)^2 \lesssim 10^{-2} \left(\frac{v_\phi}{v_H} \right)^2, \quad (4.22)$$

where in the last term we have used that $m_N < 80 \text{ GeV}$. Therefore the three-body decays to SM particles are suppressed when $m_N < m_W$ and the right-handed neutrino decays invisibly to $\nu\eta$, unless $v_\phi \gtrsim 10 v_H$. On the other hand, the coupling between the sterile neutrinos and the Majoron η is $\lambda_N = m_N/v_\phi \lesssim 0.05$ for $v_\phi \gtrsim 1.6 \text{ TeV}$, probably too small to have a significant DM annihilation cross section into NN in the first place.

Moreover, in the NN annihilation channel also light neutrinos are copiously produced, which could lead to observable signals at IceCUBE. These will depend on the neutrino energy, and therefore a detailed study of the final state spectrum is required to set constraints. Very roughly, for heavy Dark Matter we expect very energetic neutrinos, so that this scenario could be tested with current IceCUBE data, provided $E_\nu \gtrsim 100 \text{ GeV}$. If the Dark Matter is lighter, or the neutrino energy spectrum softer, DeepCore will be needed to further constrain the parameter space, since it is expected to lower the IceCUBE neutrino energy threshold to about 10 GeV .

Heavy right-handed neutrino, $m_N > m_W$: for larger values of m_N , two body decays to SM particles are open, and the corresponding widths read [24]:

$$\Gamma(N \rightarrow W^\pm \ell_\alpha^\mp) = \frac{g^2}{64\pi} |U_{\alpha N}|^2 \frac{m_N^3}{m_W^2} \left(1 - \frac{m_W^2}{m_N^2} \right)^2 \left(1 + \frac{2m_W^2}{m_N^2} \right) \quad (4.23)$$

$$\Gamma(N \rightarrow Z \nu_\alpha) = \frac{g^2}{64\pi c_W^2} |C_{\alpha N}|^2 \frac{m_N^3}{m_Z^2} \left(1 - \frac{m_Z^2}{m_N^2} \right)^2 \left(1 + \frac{2m_Z^2}{m_N^2} \right) \quad (4.24)$$

$$\Gamma(N \rightarrow h \nu_\alpha) = \frac{g^2}{64\pi} |C_{\alpha N}|^2 \frac{m_N^3}{m_W^2} \left(1 - \frac{m_h^2}{m_N^2} \right)^2 \quad (4.25)$$

In the above expressions, we have assumed that N is a Majorana fermion. From eqs. (4.14) and (4.23), we see that in this mass range the ratio between Majoron and SM particles decay widths is approximately given by

$$\frac{\Gamma(N \rightarrow \text{SM})}{\Gamma(N \rightarrow \nu\eta)} \sim \left(\frac{v_\phi}{v_H}\right)^2. \quad (4.26)$$

Thus in this mass range we expect a significant flux of gamma rays from the galactic center produced by SM annihilation products, and bounds can be set from the Fermi-LAT Space Telescope gamma ray data. A detailed study of the indirect detection signatures of our scenario is beyond the scope of this work, since Dark Matter does not decay directly to SM particles, as it is usually assumed in most analysis, but to two right-handed neutrinos that subsequently decay to them. Therefore we just estimate here the expected constraints using current analysis. See section 5 for a discussion on how these limits affect the allowed region in the parameter space of our model.

Dark matter particles in the galactic halo can scatter elastically with a nucleus and become trapped in the gravitational well of an astronomical object, such as the Sun. They will undergo subsequent scatterings, and eventually thermalize and concentrate at the core of the object. The Dark Matter accumulated in this way may annihilate into SM particles, in particular neutrinos that can be detected by neutrino experiments like IceCUBE or SuperKamiokande. However we do not discuss this type of indirect detection constraints here, since in our scenario the limits from direct searches are tighter and moreover they can always be avoided with a small enough mixing angle between the CP-even scalars, which suppresses the DM-nucleon elastic cross-section still getting the correct Dark Matter relic abundance through annihilation into NN or $\eta\rho$, which is our case.

Measurements of the cosmic microwave background (CMB) anisotropies are also sensitive to Dark Matter annihilation during the cosmic dark ages, because the injection of ionizing particles will increase the residual ionization fraction, broadening the last scattering surface and modifying the anisotropies. Under the assumption that the power deposited to the gas is directly proportional to that injected at the same redshift, with some efficiency factor f_{eff} , constraints can be placed on the combination $f_{\text{eff}}\langle\sigma v\rangle/m_{\text{DM}}$, for different SM annihilation channels in s wave. Again, the available calculations of f_{eff} assume that Dark Matter annihilates directly to a pair of SM particles, and thus they are not directly applicable to our model, but we can roughly estimate the expected impact of such limits in the allowed parameter space assuming as before that the constraints will be similar for cascade decays. In [39], f_{eff} has been calculated as a function of the Dark Matter mass for a range of SM final states, and using the most recent results from the Planck satellite she found that for any linear combination of SM final states which does not contain a significant branching ratio of Dark Matter annihilation directly into neutrinos one must have $\langle\sigma v\rangle \lesssim 3 \times 10^{-27} (m_{\text{DM}}/1 \text{ GeV}) \text{ cm}^3/\text{s}$. However in our scenario when the Dark Matter (and thus the sterile neutrino) is lighter than m_W , the final states are ν, η and therefore the above limit does not apply.

Only for higher Dark Matter masses the final annihilation products can be charged leptons and gauge bosons, but in this range the CMB limits are above the thermal relic cross section, so they do not constrain our scenario.

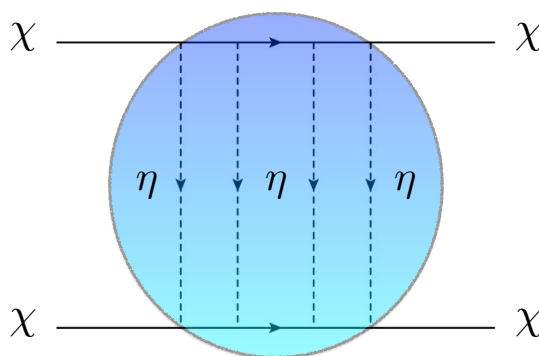


Figure 6. Diagram of self-interacting Dark Matter, via the exchange of a light pseudo-scalar.

The CMB also constrains the properties of the (massless) Majoron η , which constitutes a form of dark radiation and contribute to N_{eff} [34]. In ref. [19], it was shown that typically the limit on N_{eff} is already saturated by constraints from direct detection. In particular, for $m_\chi > 100$ GeV, a non negligible contribution to dark radiation could only happen in a small range of m_ρ from 0.5 to 1 GeV.

4.5 Self-interacting Dark Matter

The dark sector contains a light particle, the Majoron η , coupled to Dark Matter. This opens the interesting possibility of a self-interacting Dark Matter candidate due to exchanges of the light particle via diagrams such as shown in figure 6.

Self-interacting Dark Matter could explain some of the issues encountered in simulations for small-scale structure formation which assume collisionless-DM [40], and typically predict too cuspy Dark Matter profiles. Self-interacting Dark Matter could explain the lack of satellites (although introducing baryons on the simulation seems to reduce inconsistencies [41, 42]) and more importantly the *too-big-to-fail* problem [43, 44] for $\sigma_{SI}/m_\chi \sim 0.1\text{-}10$ cm^2/g .

Direct limits on self-interactions of Dark Matter are provided by lensing. From the renowned bullet cluster limit [45] to observations of other astrophysical objects, Dark Matter self interactions have been bounded in the range of $\sigma_{SI}/m_\chi < 1$ cm^2/g . Interestingly, there has been a recent claim of a measurement of self-interactions in the system Abell 3827 [46] which lies above previous upper bounds. Note that this claim has been questioned by ref. [47], which propose modifications of the former analysis leading to limits similar to the bullet cluster's.

The effect of multiple exchanges of the light particle induces an Dark Matter effective potential between two dark particles χ of spin \mathbf{s} at distance r

$$V_{\text{eff}}(r) = -\frac{\lambda_\chi^2}{4r^3 m_\chi^2} (3(\mathbf{s}_1 \cdot \hat{r})(\mathbf{s}_2 \cdot \hat{r}) - \mathbf{s}_1 \cdot \mathbf{s}_2) , \tag{4.27}$$

where we neglected terms proportional to the (possible) Majoron mass. This potential is very singular at $r \rightarrow 0$ and requires regularization. The treatment for this case is quite

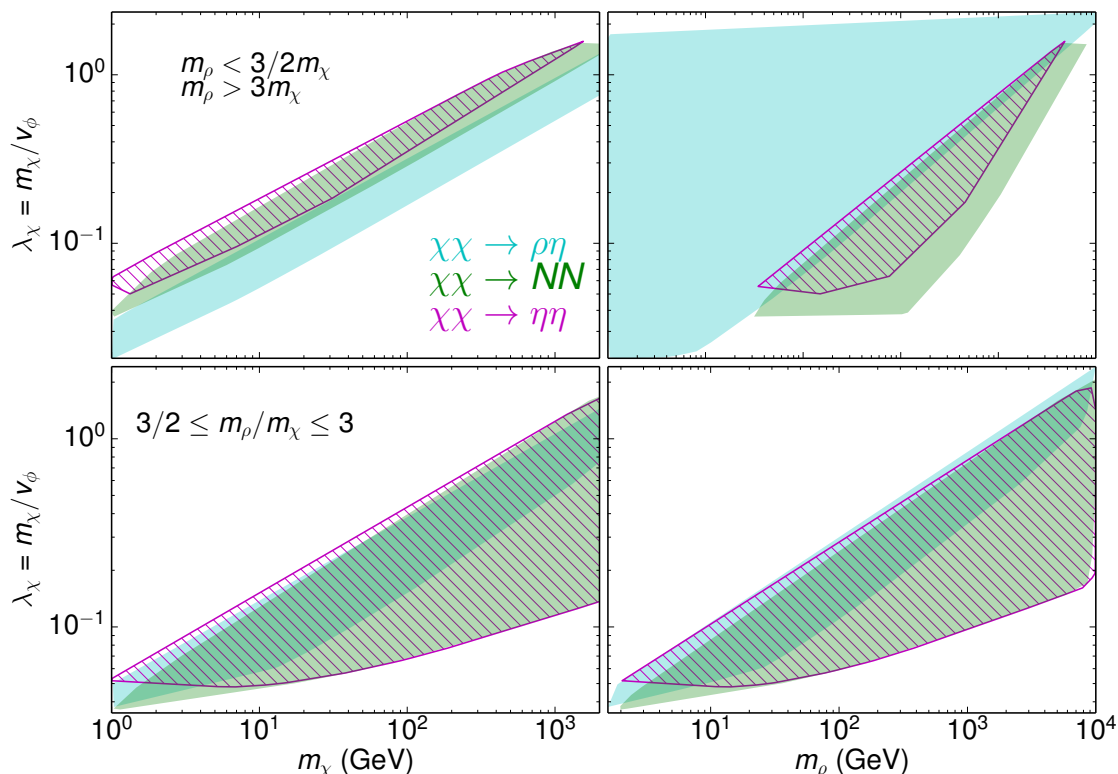


Figure 7. Coupling between the dark scalars and Dark Matter λ_χ as a function of the Dark Matter mass m_χ (left) and heavy scalar mass m_ρ (right). Outside the resonance (up) and on the resonance (down). The colors correspond to regions in parameter space in which the annihilation channel constitutes more than 60% of the total cross section for $v = 10^{-3}c$, as relevant for indirect detection.

involved, similar to a non-relativistic calculation of nucleon-nucleon interaction via the exchange of a light pion.

In the presence of these self-interactions, the annihilation cross section of a self-interacting Dark Matter would be modified respect to our discussion in section 4.3. Additional channels like $\chi\chi \rightarrow \chi\chi$ should be considered as they would be Sommerfeld-enhanced,

$$\sigma(\chi\chi \rightarrow \chi\chi)v_{\text{rel}} = S \frac{3\lambda_\chi^4}{64\pi m_\chi^2}, \tag{4.28}$$

where S is the numerical factor due to Sommerfeld enhancement. In ref. [48], numerical calculations of S at short distances were studied for this type of potential, finding that the enhancement could reach $S \sim 10^6$ for $v_{\text{rel}} = 10^{-3}$. To estimate what values of λ_χ would lead to dominance of the self-interaction dynamics via a pseudo-scalar exchange, we follow ref. [49] where the following bound is found

$$\lambda_\chi \gtrsim 0.6 \left(\frac{m_\chi}{\text{GeV}} \right)^{9/4}. \tag{4.29}$$

Note that in our model the mass of the Dark Matter particle and λ_χ are related via the dark scalar vev v_ϕ . We explored the range of these parameters leading to the correct relic

abundance and the result is shown in figure 7. The estimate in 4.29 corresponds to the upper-left corner in the left panel of this figure, away from the allowed region from the relic abundance constraint.

Moreover, there are regions of the allowed parameter space where the scalar ρ is light, and there will be exchanges of the ρ similar to those in figure 6 with ρ as a mediator. As ρ is a massive scalar mediator, the type of effective potential one would generate is Yukawa-type, with a less divergent behaviour than the pseudo-scalar. This case has been studied elsewhere, see e.g. refs. [50–54], and here we just quote the parametric dependence of the enhancement with the coupling,

$$S \sim \lambda_\chi^2 / v_{\text{rel}}, \tag{4.30}$$

for attractive potentials and $m_\rho < m_\chi$. In the right panel of figure 7 we show values of the coupling versus the mass of the mediator, finding in the region where the Sommerfeld enhancement could dominate, the self-interaction would compete with the s-wave annihilation into $\eta\rho$. Note that a similar enhancement could happen in the channels of annihilation to right-handed neutrinos. Indeed, one could exchange light η or ρ mediators as in figure 6, but now between the Dark Matter particle and N .

We conclude that the effects of self-interactions via the exchange of a pseudo-scalar mediator do not affect our model based on a naive estimate, but the effect of scalar exchanges and impact on the annihilation of Dark Matter into right-handed neutrinos deserve further study.

5 Results

In this section we show how the constraints discussed in the previous sections affect the parameter space of our model, described by m_χ, m_N, m_ρ and the Yukawa coupling λ_χ , which fixes $v_\phi = m_\chi / \lambda_\chi$.

As discussed in section 4.4 the annihilation product of the Dark Matter particle may lead to sizeable imprints on FermiLAT or HESS or the CMB due to the emission of photons and the re-ionization power of the products of the annihilation respectively. The annihilation channels that can lead a significant signature are to right-handed neutrinos $\chi\chi \rightarrow NN$ with $NN \rightarrow W^+W^- + \text{leptons}$, whenever $m_\chi > m_W$. A precise analysis of these decay channels would require a simulation of the photon spectrum from these cascade decays, such as performed in ref. [55]. Instead, we naively show the actual bounds for a 2 to 2 process in figure 8.

Apart from signatures from gamma-rays, in our model neutrinos are typically produced in Dark Matter annihilation, leading to a flux from dense regions of Dark Matter or energy injection into the CMB. Indeed, when the right-handed neutrino channel dominates, numerous neutrinos will be produced in the annihilations. IceCUBE can constrain the cross section to neutrinos measuring the flux from nearby Galaxies and Clusters (NG) [58], the Galactic Halo (GH) [59] and the Galactic Center (GC) [60] and the CMB [39] can constrain the annihilation cross section to neutrinos from the impact on re-ionization due

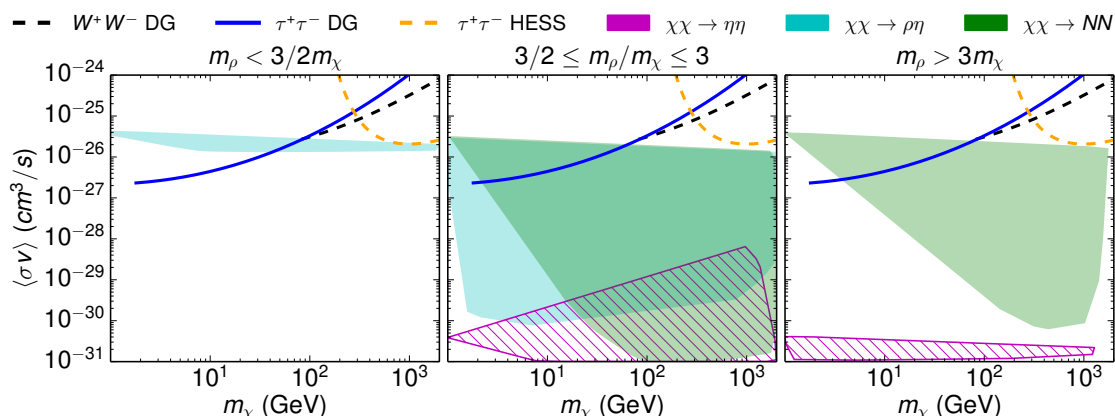


Figure 8. Annihilation cross section at $v = 10^{-3}c$ as a function of the Dark Matter mass as relevant for indirect detection. The color bands account for regions of parameter space in which the indicated annihilation channel provides more than 60% of the total cross section. Also shown in this plot exclusion curves from FermiLAT dwarf galaxies (DG) [56] and HESS galactic center (GC) [57].

to electroweak corrections. However, currently these probes lie three orders of magnitude above the model prediction, and thus cannot place a constrain on the model.

It has been noted that for Dark Matter masses above 200 GeV annihilating into a pair of light neutrinos, Fermi-LAT data on gamma-rays sets the most stringent constraints on the annihilation cross-section [61]. In principle, there would be similar limits in our scenario, but such a heavy Dark Matter will also produce W bosons and leptons, which lead to stronger bounds discussed above.

In figure 8 we summarize these results in the plane of annihilation cross section into a particular final state versus the Dark Matter mass for the three kinematical regions of interest. The colored contours correspond to regions with dominance of one channel in the relic abundance, either to dark scalars or right-handed neutrinos. As argued in section 4.4 the annihilation products from the channels $\chi\chi \rightarrow \rho\eta$ and $\chi\chi \rightarrow \eta\eta$ cannot be constrained since the ρ decays to two η 's, which are invisible.

Therefore the only limits that apply are those related to annihilation into right-handed neutrinos, which is suppressed by m_N^2/m_χ^2 . Promising signatures of these decays can be obtained when right-handed neutrinos undergo two-body decays in W and charged leptons or neutrinos in association with a Higgs or a Z boson, see eq. (4.23), and hence restricted to $m_\chi > m_W$. On the other hand, for low Dark Matter mass only sterile neutrinos with $m_N < m_W$ can be produced and the dominant decay $N \rightarrow \nu\eta$ is unobservable, see section 4.4. Finally, note that the diagonal feature on the green region in the right panel is due to the fact that in the scan we have considered a minimum of 1 GeV for m_N .

From these results one can conclude that the model is currently unconstrained from indirect detection once other limits are taken into account, although the prospects for future experiments deserve a detailed study.

Notice that in the absence of the global $U(1)_{B-L}$ symmetry the conclusions could be quite different. First, the sterile neutrino mass would be independent of its coupling, λ_N ,

and there would not be any suppression of the annihilation cross section when $m_N \ll m_\chi$. Moreover, since in our case the Majoron is a Goldstone boson, it is expected to be lighter than the other scalars in the theory, and one can neglect its mass and assume that all possible annihilation and decay channels into Majorons are always kinematically allowed. However if the lepton number symmetry were explicitly broken, generically the real and imaginary components of ϕ would have similar masses, leading to cases where the channel into pseudo-scalars could be kinematically closed.

In summary, on the one hand the scenario we have considered with spontaneously broken $U(1)_{B-L}$ is more constrained than the one with explicit breaking, due to relation between sterile neutrino masses and couplings to ϕ . On the other hand, if there was no symmetry, we generically would expect a heavier pseudo-scalar, which could lead to the closing of some invisible channels into Majorons. In this case, constraints from the invisible Higgs decay width would be absent, Dark Matter would only annihilate into sterile neutrinos, and the decay $N \rightarrow \nu\eta$ would not occur. Therefore limits from indirect searches, in particular the curve from Fermi-LAT dwarf galaxies on $\tau\tau$ shown in figure 8, would apply to low Dark Matter mass $\lesssim m_W$.

6 Conclusions and outlook

In this paper we have studied a simple case connecting Dark Matter and the origin of neutrino masses, where the link to the Standard Model is dictated by a global $U(1)_{B-L}$ symmetry. In our model, the dark sector contains fermions, Dark Matter and right-handed neutrinos, and a complex scalar which plays the dual role of generating Majorana masses for the dark fermions and communicating with the Higgs via a Higgs portal coupling. The stability of the Dark Matter fermion can be due to an additional dark sector symmetry, compositeness or exotic lepton number.

After spontaneous electroweak and $U(1)_{B-L}$ symmetry breaking, the Higgs and dark scalar mix. This mixing is very constrained by bounds on the invisible width of the Higgs from the LHC and by LUX via the induced coupling of Dark Matter to the Higgs.

We then focused on other aspects of the phenomenology of this model, assuming that the stable dark fermion constitutes the main component of Dark Matter in the Universe. Due to the presence of right-handed fermions and a complex scalar in the dark sector, there is an interplay between Dark Matter annihilation to both types of particles. Dark Matter annihilation to right-handed neutrinos could dominate at freeze-out provided the scalar is heavy. And, even when Dark Matter annihilation to Majorons dominated the dynamics at freeze-out, we found that the annihilation to heavy neutrinos could control today's indirect detection signatures.

Moreover, we found a very interesting phenomenology reaching from possible signatures at colliders via exotic Higgs decays, to effects on gamma-rays from right-handed neutrino production and decays to charged particles. In this paper, we did not try to accommodate a possible excess in the gamma-ray spectrum, instead used bounds from 2-to-2 scattering, adapted to our case in a relatively naive fashion. A proper study of the spectrum of

gamma-rays in our model is beyond the scope of this paper, but certainly deserves further investigation since the estimated bounds are close to the WIMP thermal cross section.

Additionally, we noted that the presence of neutrinos in decay channels could be probed in the future via neutrino telescopes and more precise studies of the CMB, but that at the moment the limits are much weaker than any other annihilations involving charged particles.

Finally, we briefly discussed the possibility of strong self-interactions of Dark Matter due to the exchange of the dark scalar. We found that Majoron exchange cannot dominate the Dark Matter dynamics, but the effect of exchanges of the dark scalar component deserves further study.

Acknowledgments

We thank Pilar Hernández, Laura Lopez-Honorez, Olga Mena, Sergio Palomares Ruiz, Roberto Ruiz de Austri, Jordi Salvadó and Sam Witte for illuminating discussions. ME specially thanks Antonia Abenza for inspiring and encouraging conversations. This work has been partially supported by the European Union's Horizon 2020 research and innovation programme under the Marie Skłodowska-Curie grant agreements No 674896 and 690575, by the Spanish MINECO under grants FPA2014-57816-P and SEV-2014-0398, and by Generalitat Valenciana grant PROMETEO/2014/050. ME is supported by Spanish Grant FPU13/03111 of MECD. NR thanks the Department of Physics and Astronomy in the University of Sussex for the warm hospitality. The work of VS is supported by the Science Technology and Facilities Council (STFC) under grant number ST/J000477/1.

Open Access. This article is distributed under the terms of the Creative Commons Attribution License ([CC-BY 4.0](https://creativecommons.org/licenses/by/4.0/)), which permits any use, distribution and reproduction in any medium, provided the original author(s) and source are credited.

References

- [1] S. Dodelson and L.M. Widrow, *Sterile-neutrinos as dark matter*, *Phys. Rev. Lett.* **72** (1994) 17 [[hep-ph/9303287](https://arxiv.org/abs/hep-ph/9303287)] [[INSPIRE](#)].
- [2] R. Adhikari et al., *A white paper on keV sterile neutrino dark matter*, [arXiv:1602.04816](https://arxiv.org/abs/1602.04816) [[INSPIRE](#)].
- [3] V. Gonzalez Macias and J. Wudka, *Effective theories for dark matter interactions and the neutrino portal paradigm*, *JHEP* **07** (2015) 161 [[arXiv:1506.03825](https://arxiv.org/abs/1506.03825)] [[INSPIRE](#)].
- [4] V. González-Macías, J.I. Illana and J. Wudka, *A realistic model for dark matter interactions in the neutrino portal paradigm*, *JHEP* **05** (2016) 171 [[arXiv:1601.05051](https://arxiv.org/abs/1601.05051)] [[INSPIRE](#)].
- [5] M. Escudero, N. Rius and V. Sanz, *Sterile neutrino portal to dark matter II: exact dark symmetry*, [arXiv:1607.02373](https://arxiv.org/abs/1607.02373) [[INSPIRE](#)].
- [6] Y. Chikashige, R.N. Mohapatra and R.D. Peccei, *Are there real Goldstone bosons associated with broken lepton number?*, *Phys. Lett.* **B 98** (1981) 265 [[INSPIRE](#)].

- [7] S. Khalil, *Low scale B-L extension of the Standard Model at the LHC*, *J. Phys. G* **35** (2008) 055001 [[hep-ph/0611205](#)] [[INSPIRE](#)].
- [8] S. Iso, N. Okada and Y. Orikasa, *Classically conformal B-L extended Standard Model*, *Phys. Lett. B* **676** (2009) 81 [[arXiv:0902.4050](#)] [[INSPIRE](#)].
- [9] S. Kanemura, T. Matsui and H. Sugiyama, *Neutrino mass and dark matter from gauged $U(1)_{B-L}$ breaking*, *Phys. Rev. D* **90** (2014) 013001 [[arXiv:1405.1935](#)] [[INSPIRE](#)].
- [10] N. Arkani-Hamed, S. Dimopoulos, G.R. Dvali and J. March-Russell, *Neutrino masses from large extra dimensions*, *Phys. Rev. D* **65** (2001) 024032 [[hep-ph/9811448](#)] [[INSPIRE](#)].
- [11] N. Arkani-Hamed and M. Schmaltz, *Hierarchies without symmetries from extra dimensions*, *Phys. Rev. D* **61** (2000) 033005 [[hep-ph/9903417](#)] [[INSPIRE](#)].
- [12] Y. Grossman and M. Neubert, *Neutrino masses and mixings in nonfactorizable geometry*, *Phys. Lett. B* **474** (2000) 361 [[hep-ph/9912408](#)] [[INSPIRE](#)].
- [13] M. Lindner, D. Schmidt and T. Schwetz, *Dark matter and neutrino masses from global $U(1)_{B-L}$ symmetry breaking*, *Phys. Lett. B* **705** (2011) 324 [[arXiv:1105.4626](#)] [[INSPIRE](#)].
- [14] J. Schechter and J.W.F. Valle, *Neutrino decay and spontaneous violation of lepton number*, *Phys. Rev. D* **25** (1982) 774 [[INSPIRE](#)].
- [15] S.R. Coleman, *Why there is nothing rather than something: a theory of the cosmological constant*, *Nucl. Phys. B* **310** (1988) 643 [[INSPIRE](#)].
- [16] E.K. Akhmedov, Z.G. Berezhiani, R.N. Mohapatra and G. Senjanović, *Planck scale effects on the majoron*, *Phys. Lett. B* **299** (1993) 90 [[hep-ph/9209285](#)] [[INSPIRE](#)].
- [17] M. Lattanzi, R.A. Lineros and M. Taoso, *Connecting neutrino physics with dark matter*, *New J. Phys.* **16** (2014) 125012 [[arXiv:1406.0004](#)] [[INSPIRE](#)].
- [18] F. Bazzocchi, M. Lattanzi, S. Riemer-Sørensen and J.W.F. Valle, *X-ray photons from late-decaying majoron dark matter*, *JCAP* **08** (2008) 013 [[arXiv:0805.2372](#)] [[INSPIRE](#)].
- [19] C. Garcia-Cely, A. Ibarra and E. Molinaro, *Cosmological and astrophysical signatures of dark matter annihilations into pseudo-Goldstone bosons*, *JCAP* **02** (2014) 032 [[arXiv:1312.3578](#)] [[INSPIRE](#)].
- [20] M. Carena, A. Daleo, B.A. Dobrescu and T.M.P. Tait, *Z' gauge bosons at the Tevatron*, *Phys. Rev. D* **70** (2004) 093009 [[hep-ph/0408098](#)] [[INSPIRE](#)].
- [21] N. Okada and O. Seto, *Higgs portal dark matter in the minimal gauged $U(1)_{B-L}$ model*, *Phys. Rev. D* **82** (2010) 023507 [[arXiv:1002.2525](#)] [[INSPIRE](#)].
- [22] A. De Simone, V. Sanz and H.P. Sato, *Pseudo-Dirac dark matter leaves a trace*, *Phys. Rev. Lett.* **105** (2010) 121802 [[arXiv:1004.1567](#)] [[INSPIRE](#)].
- [23] J. Racker and N. Rius, *Helicogenesis: WIMPy baryogenesis with sterile neutrinos and other realizations*, *JHEP* **11** (2014) 163 [[arXiv:1406.6105](#)] [[INSPIRE](#)].
- [24] A. Pilaftsis, *Radiatively induced neutrino masses and large Higgs neutrino couplings in the Standard Model with Majorana fields*, *Z. Phys. C* **55** (1992) 275 [[hep-ph/9901206](#)] [[INSPIRE](#)].
- [25] LUX collaboration, D.S. Akerib et al., *The Large Underground Xenon (LUX) experiment*, *Nucl. Instrum. Meth. A* **704** (2013) 111 [[arXiv:1211.3788](#)] [[INSPIRE](#)].

- [42] O.Y. Gnedin, A.V. Kravtsov, A.A. Klypin and D. Nagai, *Response of dark matter halos to condensation of baryons: cosmological simulations and improved adiabatic contraction model*, *Astrophys. J.* **616** (2004) 16 [[astro-ph/0406247](#)] [[INSPIRE](#)].
- [43] T. Sawala, Q. Guo, C. Scannapieco, A. Jenkins and S.D.M. White, *What is the (dark) matter with dwarf galaxies?*, *Mon. Not. Roy. Astron. Soc.* **413** (2011) 659 [[arXiv:1003.0671](#)] [[INSPIRE](#)].
- [44] M. Boylan-Kolchin, J.S. Bullock and M. Kaplinghat, *Too big to fail? The puzzling darkness of massive Milky Way subhaloes*, *Mon. Not. Roy. Astron. Soc.* **415** (2011) L40 [[arXiv:1103.0007](#)] [[INSPIRE](#)].
- [45] M. Markevitch et al., *Direct constraints on the dark matter self-interaction cross-section from the merging galaxy cluster 1E0657-56*, *Astrophys. J.* **606** (2004) 819 [[astro-ph/0309303](#)] [[INSPIRE](#)].
- [46] R. Massey et al., *The behaviour of dark matter associated with four bright cluster galaxies in the 10 kpc core of Abell 3827*, *Mon. Not. Roy. Astron. Soc.* **449** (2015) 3393 [[arXiv:1504.03388](#)] [[INSPIRE](#)].
- [47] F. Kahlhoefer, K. Schmidt-Hoberg, J. Kummer and S. Sarkar, *On the interpretation of dark matter self-interactions in Abell 3827*, *Mon. Not. Roy. Astron. Soc.* **452** (2015) L54 [[arXiv:1504.06576](#)] [[INSPIRE](#)].
- [48] B. Bellazzini, M. Cliche and P. Tanedo, *Effective theory of self-interacting dark matter*, *Phys. Rev. D* **88** (2013) 083506 [[arXiv:1307.1129](#)] [[INSPIRE](#)].
- [49] M. Archidiacono, S. Hannestad, R.S. Hansen and T. Tram, *Cosmology with self-interacting sterile neutrinos and dark matter — a pseudoscalar model*, *Phys. Rev. D* **91** (2015) 065021 [[arXiv:1404.5915](#)] [[INSPIRE](#)].
- [50] R. Iengo, *Sommerfeld enhancement: general results from field theory diagrams*, *JHEP* **05** (2009) 024 [[arXiv:0902.0688](#)] [[INSPIRE](#)].
- [51] S. Cassel, *Sommerfeld factor for arbitrary partial wave processes*, *J. Phys. G* **37** (2010) 105009 [[arXiv:0903.5307](#)] [[INSPIRE](#)].
- [52] M. Cirelli, A. Strumia and M. Tamburini, *Cosmology and astrophysics of minimal dark matter*, *Nucl. Phys. B* **787** (2007) 152 [[arXiv:0706.4071](#)] [[INSPIRE](#)].
- [53] L. Lopez-Honorez, T. Schwetz and J. Zupan, *Higgs portal, fermionic dark matter and a Standard Model like Higgs at 125 GeV*, *Phys. Lett. B* **716** (2012) 179 [[arXiv:1203.2064](#)] [[INSPIRE](#)].
- [54] M. Lisanti, *Lectures on dark matter physics*, in *Theoretical Advanced Study Institute in Elementary Particle Physics: New Frontiers in Fields and Strings (TASI 2015)*, Boulder U.S.A., 1–26 June 2015 [[arXiv:1603.03797](#)] [[INSPIRE](#)].
- [55] C. Garcia-Cely and J. Heeck, *Indirect searches of dark matter via polynomial spectral features*, *JCAP* **08** (2016) 023 [[arXiv:1605.08049](#)] [[INSPIRE](#)].
- [56] FERMI-LAT collaboration, M. Ackermann et al., *Searching for dark matter annihilation from Milky Way dwarf spheroidal galaxies with six years of Fermi Large Area Telescope data*, *Phys. Rev. Lett.* **115** (2015) 231301 [[arXiv:1503.02641](#)] [[INSPIRE](#)].
- [57] HESS collaboration, H. Abdallah et al., *Search for dark matter annihilations towards the inner galactic halo from 10 years of observations with H.E.S.S.*, *Phys. Rev. Lett.* **117** (2016) 111301 [[arXiv:1607.08142](#)] [[INSPIRE](#)].

